2023-12-12

Characterizing Quirky Signals

Joshua D. Forsyth
Brigham Young University

Characterizing Quirky Signals

Joshua D. Forsyth

A thesis submitted to the faculty of
Brigham Young University
in partial fulfillment of the requirements for the degree of

Master of Science

Christopher Verhaaren, Chair
Eric Hirschmann
Branton Campbell

Department of Physics and Astronomy

Brigham Young University

ABSTRACT

Characterizing Quirky Signals

Joshua D. Forsyth
Department of Physics and Astronomy, BYU
Master of Science

Large collider facilities such as the Large Hadron Collider (LHC) employ a variety of search methods in hopes of finding new particles. It may be that new physics beyond the SM is waiting to be discovered at energies accessible to the LHC. Quirks are particles charged under a new confining gauge group with masses much larger than their confinement scale. This project details the dynamics of quirks, as well as the production and decay of electrically charged bound states of scalar quirks. The cross section for these states is compared to existing $W\gamma$ resonance searches at the LHC. Such a state is above the most sensitive LHC search up to an invariant mass of about $M \lesssim 640$ GeV.

Keywords: quirks, squirks, LHC, BSM physics

ACKNOWLEDGMENTS

Thank you to Dr. Chris Verhaaren for teaching me along the way. Also, special thanks to my wife, Kelsey, for supporting me throughout this project and especially during the writing process.

Contents

Table of Contents **iv**

List of Figures **v**

1 Introduction **1**
1.1 Beyond the Standard Model 1
1.2 LHC Discovery Potential 2
1.3 Higgs Boson and Electroweak Hierarchy 3
1.4 Neutral Naturalness 4

2 Quirks **6**
2.1 Parton Showers 7
2.2 Quirk Dynamics 10
2.2.1 Photon Emission 12
2.2.2 Glueball Emission 14

3 Production Calculations **16**
3.1 Production Cross Sections 16
3.2 Parton Distribution Functions 19

4 Decay and Experimental Searches **21**
4.1 Beta Decay 21
4.2 Branching Ratios 24
4.2.1 Search Signals 26
4.2.2 Other Signals 29
4.3 Resonance Searches at the LHC 30

5 Conclusions and Future Work **32**

Bibliography **34**

List of Figures

2.1 (top) A parton-antiparton pair, called a meson, connected by a color flux tube of length ℓ. (bottom) Two mesons with the inner partons separated by $\Delta\ell_q \sim \frac{1}{2m_q}$. 8

2.2 A collision event at the LHC leading to the discovery of the Higgs boson. The orange lines are jets produced through parton pair production. Image taken from: https://home.cern/resources/image/physics/higgs-collection-images-gallery. . 9

3.1 Leading-order Feynman diagram for positively charged squirkonium production. 17

4.1 Three-body decay for a $\widetilde{u}$ squirk at tree-level. A similar diagram can be computed for the decay of the $\widetilde{d}$ squirk. 22

4.2 Branching ratios for squirkonium decay at low angular momentum with mass splittings $\Delta = 0$, $\Delta = \frac{m_w}{2}$, and $\Delta = m_w$. 25

4.3 The four tree-level diagrams contributing to positively charged squirkonium decaying into $W^+ + \gamma$. 26

4.4 Only the s-channel contributes at tree-level to charged squirkonium decay into fermions. 30

4.5 LHC resonance searches for the $W\gamma$ signal with the production cross section for squirks overlaid. 31

Chapter 1

Introduction

1.1 Beyond the Standard Model

The crowning achievement of particle physics was the completion of the Standard Model (SM). The model consists of the most basic building blocks of matter in the observable universe and how they interact with each other. We call these building blocks particles—quantum fluctuations of classical fields that extend throughout spacetime. The SM groups these particles according to their quantum numbers which have been measured by experiment. It very accurately accounts for nearly all the small scale physics that we can measure. This includes electromagnetism, beta decay of an atomic nucleus, and how protons and neutrons are formed. For example, the value of the fine-structure constant, $\alpha \approx \frac{1}{137}$, in electrodynamics has been found through various high-precision tests to agree to within ten parts per billion, or 10^{-8}. At larger scales, such as at the cellular level or even the world as seen by humans, the interactions of these particles include the fundamental forces of nature. However, several observed phenomena indicate that there are aspects of nature for which the SM offers no explanations.

At low energy scales, the SM only accounts for interactions for three of the four fundamental forces: the strong and weak nuclear forces and electromagnetism. As one moves to higher energy scales (such as moving to the classical regime), the SM does not describe how matter interacts through gravitational fields. Since gravity is perhaps the most notable fundamental force in everyday life, many hope to find a theory that unifies the four fundamental forces. Another example of something that the SM does not address is the origin of neutrino masses. While the SM does incorporate three generations of neutrinos, it is completely agnostic about the values and origin of neutrino masses. However, the 2015 Nobel Prize in Physics was awarded to Takaaki Kajita and Arthur B. McDonald "for the discovery of neutrino oscillations, which shows that neutrinos have mass."[1] These quantum gravity and neutrino mass problems hint at the need for physics beyond the Standard Model (BSM). Other problems that indicate a need for BSM include the identity of dark matter, why there is more matter than antimatter in the universe, and the electroweak hierarchy problem—which is discussed in Section 1.3. With all of these unanswered questions, it is no wonder that people continue searching for new particles from cosmological sources and at colliders.

1.2 LHC Discovery Potential

The Large Hadron Collider (LHC) is currently the world's largest collider facility, located in Geneva, Switzerland. It continues to break records for energy achieved in collisions, currently operating at a center-of-mass energy of 13.6 TeV (or 13.6×10^{12} eV). While it continues to probe the highest energies accessible to particle detectors, the question remains if the search potential of this facility is being fully realized.

[1]The Nobel Prize in Physics 2015. https://www.nobelprize.org/prizes/physics/2015/summary/

As of May 2022, the LHC collides roughly 1 billion protons per second, but only keeps $\sim 6 \times 10^{-5}\%$ of the collision data[2]. This is because (i) many of the protons simply bounce off each other and (ii) a lot of the data that hits the detectors comes from jets of quarks (more on this in Chapter 2). While it is true that many of the events that get discarded are not interesting (e.g. elastic collisions of the protons), there may be events that do not pass the triggers employed by the detectors yet correspond to processes involving new particles. There could be states at energies already accessible to the LHC that are being missed. This is a major motivation for this research.

1.3 Higgs Boson and Electroweak Hierarchy

Another motivation for this project includes the last piece of the SM that was discovered, the Higgs boson [1, 2] (or "Higgs"). The Higgs is special because it is spin-0; it is the only scalar field in the SM. Hence, the field has no preferred orientation in space. As such, the Higgs field can have a nonzero ground state value without breaking Lorentz invariance—a symmetry related to special relativity that is fundamental to particle physics. This ground state value is called the vacuum expectation value (VEV) of the Higgs field.

One consequence of this nonzero VEV is that it gives mass to most of the other particles in the SM. Another is that, in the absence of special structure, one would generally expect the Higgs' VEV to be on the order of the highest scale to which it couples. The mass of the Higgs (and hence its VEV) is some finite value that can be measured. In quantum field theory (QFT), this mass comes from a series of loops in the Higgs propagator. Each loop introduces divergences which are on this highest scale. The scale at which objects couple gravitationally is called the Planck scale. If the SM is correct up to this scale, $m_{\text{Pl}} \sim 10^{19}$ GeV, the VEV should be around that scale. Instead, the value of the Higgs' VEV is $v = 173$

[2]See, for example, the ATLAS detector statistics, see https://atlas.cern/Discover/Detector/Trigger-DAQ

GeV, so the ratio between v and the Planck scale is

$$\frac{v}{m_{\rm Pl}} \sim 10^{-17} \ .$$

This tiny ratio is known as the electroweak hierarchy problem and is a primary motivation for this project. Many symmetry-based extensions of the SM have been explored to address this hierarchy problem.

It may be that a new global symmetry ensures that the Higgs' VEV is insensitive to higher energy scales. Typically, this new symmetry is only approximate so that the value of the Higgs VEV is controlled to the degree by which the symmetry is preserved. For instance, suppose the symmetry is preserved by the entire theory except for one operator in the Lagrangian, whose coefficient is small. This small violation of the symmetry allows the hierarchy between the Higgs VEV and other scales to be understood. In contrast, if operators that violate the symmetry have large coefficients, then the hierarchy problem remains.

1.4 Neutral Naturalness

Within the SM, the particle with the largest coupling to the Higgs is the top quark, with a Yukawa coupling $\lambda_t \approx 1$. Consequently, any new symmetry must incorporate the top quark to properly address the electroweak hierarchy. In such a framework the top quark will be related by this new symmetry to particles not yet discovered, referred to as top partners.

In the simplest manifestations of this idea, these partners are charged under SM color. In such a scenario, evidence of these particles would be expected to appear in experiments at the LHC. So far, however, experiments have probed up to about 1.3 TeV in top partner mass without finding evidence of such particles [3–5]. Even before the LHC turned on, the possibility of colorless top partners began to be explored.

Naturalness is the fundamental idea that the value of the Higgs VEV is not finely tuned, but includes natural corrections to divergences that arise from loops in the Higgs propagator in quantum field theory [6]. The term "neutral naturalness" is used to describe solutions to the hierarchy problem within the naturalness framework in which the top partners are QCD color neutral [7]. Some models that fall under this framework predict states charged under a new confining gauge group with masses much higher than their confining scale—the energy at which the particles remain bound.[3] One such model is Folded Supersymmetry (or Folded SUSY) [8], which extends the group structure of the SM to $SU(3)_{\mathrm{QCD}'} \times SU(3)_{\mathrm{QCD}} \times SU(2)_{\mathrm{L}} \times U(1)_{\mathrm{Y}}$. Folded SUSY and other neutral natural models can allow for the existence of quirks.

[3]Such states are called "quirks" and will be discussed in more detail in the next chapter.

Chapter 2

Quirks

To understand the basic principles that describe what a quirk is, it is most beneficial to first understand how quarks in the SM can pair produce. Such pair production leads to jets, which constitute most of the data that the LHC collects. The idea behind quirks was described by [9, 10]. However, the more recent phenomenological investigation was begun by [11]. The quirks described in this work are motivated by neutral naturalness, i.e. they help naturally correct the Higgs VEV (the electroweak hierarchy problem described in the last chapter) and are not charged under SM color. However, quirks in general will be introduced in the following sections.

This chapter will begin with a review of SM pair production. Next will be a description and summary of quirks and quirk dynamics as it exists in the literature, with a more careful consideration of relativistic effects. After describing the dynamics of quirks in a bound state, two distinct types of radiation will be considered—the emission of photons and of hidden glueballs. This will provide an idea of the likelihood that a bound quirk pair will radiate and how quickly the pair will de-excite before decay.

2.1 Parton Showers

It has long been known that protons are not fundamental particles [12, 13]. While we commonly call the constituents of hadrons (e.g. protons, neutrons, and the like) "quarks", Richard Feynman first called them "partons". Among other quantum numbers, these partons have a "color charge" under the $SU(3)$ gauge group that describes quantum chromodynamics (QCD), or the strong force at the level of individual particles. How strongly partons couple to the gluon field, α_s, varies with energy. When α_s is small, how it changes with energy can be calculated perturbatively at some energy scale Q as[1]

$$\alpha_s(Q) = \frac{\alpha_s(Q_0)}{1 + \frac{\alpha_s(Q_0)}{2\pi}\left(11 - \frac{2}{3}n_f\right)\ln\frac{Q}{Q_0}} \ , \tag{2.1.1}$$

where Q_0 is some reference energy measured by experiment and n_f is the number of particles with QCD charge with mass smaller than Q. We note that for $Q > Q_0$, the denominator is larger than one and increases with Q, so α_s decreases as energy increases. At some energy, Λ_{QCD}, this coupling becomes infinite, so $\alpha_s(\Lambda_{\text{QCD}}) \to \infty$. This means that α_s is too large to be calculated perturbatively, so this is taken to signify the phase transition to bound quarks and gluons. Hence, this value Λ_{QCD} is called the confinement scale.

Determining how the bound state evolves with time involves treating the system semi-classically since the coupling cannot be computed perturbatively. A system of two bound partons can be modeled as two particles joined by a "tube" (or "string") of color charge, with a linear potential [15, 16]

$$V_{\text{QCD}} \approx \sigma r \ , \tag{2.1.2}$$

where σ is called the "string tension". This naming comes by computing the force that the string exerts on the partons

$$F_{\text{QCD}} = -\nabla V_{\text{QCD}} \approx -\sigma \ . \tag{2.1.3}$$

[1]This equation is for one-loop corrections. See Problem 17.1 in [14] for finding the two-loop corrected formula.

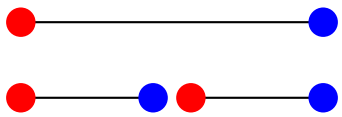

Figure 2.1 (top) A parton-antiparton pair, called a meson, connected by a color flux tube of length ℓ. (bottom) Two mesons with the inner partons separated by $\Delta\ell_q \sim \frac{1}{2m_q}$.

In natural units (where $c = \hbar = 1$), force has units of energy squared, so σ must also have those units. Since the Λ_{QCD} is the only energy scale related to confinement, it must be that $\sigma \sim \Lambda^2_{\text{QCD}}$ by dimensional analysis. Lattice QCD calculations have found that $\sigma \approx 3.6\Lambda^2_{\text{QCD}}$ [17, 18]. Noting this, the energy of a bound parton-antiparton pair, each with mass m_q and connected by a tube of length ℓ, is given by

$$E_1 \approx 2m_q + E_{\text{string},\,1} = 2m_q + \Lambda^2_{\text{QCD}}\ell \ . \tag{2.1.4}$$

This energy can be compared to a string that has fragmented to allow for the production of another two partons, as seen in Figure 2.1.

Because the energy at which the partons can be produced corresponds to a particular length scale, the minimal separation distance between the produced partons is $\Delta\ell_q \sim \frac{1}{2m_q}$. Then the fragmented string system would have energy

$$E_2 \approx 4m_q + E_{\text{string},\,2} = 4m_q + \Lambda^2_{\text{QCD}}\left(\ell - \frac{1}{2m_q}\right) \ . \tag{2.1.5}$$

Taking the difference in energies of the two systems,

$$\Delta E = E_1 - E_2 \approx \frac{\Lambda^2_{\text{QCD}}}{2m_q} - 2m_q = 2m_q\left(\frac{\Lambda^2_{\text{QCD}}}{4m_q^2} - 1\right) \ , \tag{2.1.6}$$

which means that $\Delta E > 0$ whenever $\Lambda_{\text{QCD}} > 2m_q$. The world average measured value for the confinement scale (assuming only three quark flavors) is $\Lambda_{\text{QCD}} = 332 \pm 17$ MeV [19]. Of the six SM quarks that have been experimentally measured, three of them have masses below this scale: the up ($m_q = 2.16$ MeV), the down ($m_q = 4.67$ MeV), and the strange ($m_q = 93$ MeV)

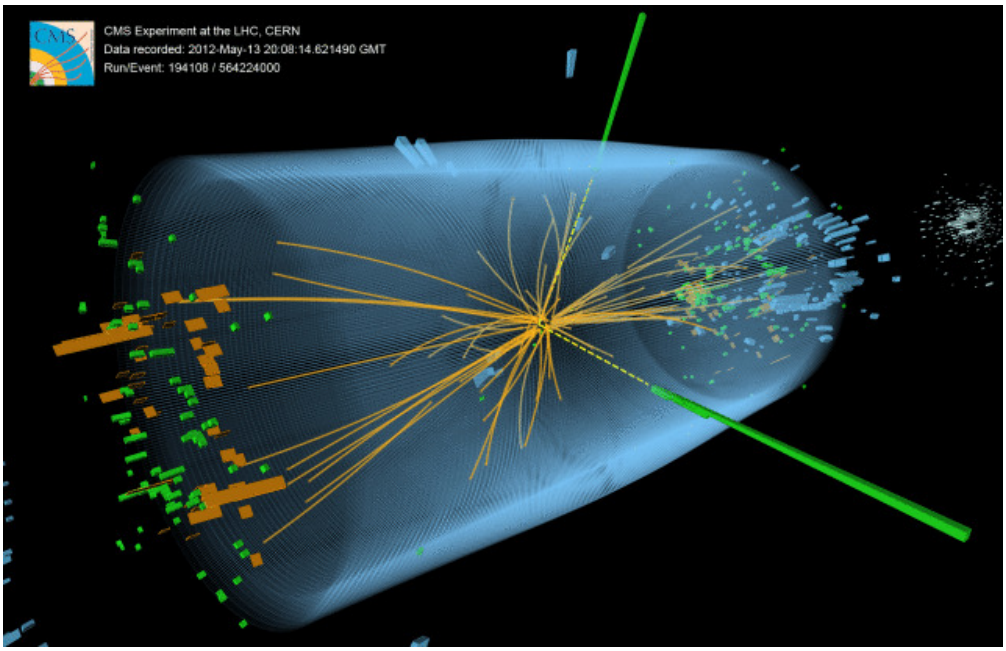

Figure 2.2 A collision event at the LHC leading to the discovery of the Higgs boson. The orange lines are jets produced through parton pair production. Image taken from: https://home.cern/resources/image/physics/higgs-collection-images-gallery.

quarks. Hence, in proton-proton collisions at the LHC and other at other hadron colliders, it is energetically favorable for pair production to occur. Since collisions occur at high energies, this phenomenon leads to large chains of produced pairs which appear as jets to the detectors.

While this may seem strange in a classical sense, jets are nevertheless the bulk of the signals seen at hadron colliders like the LHC. Therefore, for SM particles charged under a confining gauge group, pair production is the norm. This begs the question: what if there were BSM states in which pair production was not normal, but highly suppressed? It is this concept that motivated the development of quirk models.

2.2 Quirk Dynamics

Quirks were first proposed by [9, 10], though called by a different name. More recently, [11] coined the term "quirks" and outlined their phenomenology within colliders. What follows in this section in an update to the former's analysis of quirk dynamics including relativistic effects.

When particles experiencing a confining gauge theory (call it QCD$'$) are produced one can consider them as connected by a tube of color flux as in normal QCD. They can likewsie be thought of as experiencing a confining, linear potential, similar to that of Eqn. (2.1.2), with a new string tension σ' related to the scale of confinement by $\sigma' \approx 3.6\Lambda^2_{\text{QCD}'}$. When the theory includes states with masses below the confinement scale, the same analysis from Section 2.1 applies, and pair production can occur, causing the string to fragment into jets of hadrons.

If there are no states lighter than the confinement scale in the confining gauge group, then the probability of pair production is exponentially suppressed, as shown in [11]. Schwinger pair production (per volume) of particles with mass m_q in an electric field E yields

$$\frac{\Gamma}{V} = \frac{E^2}{4\pi^3} e^{-\pi m_q^2/E} \ . \tag{2.2.1}$$

Because the gauge field flux is confined to a tube, the energy density per length is the string tension (σ'). It is related to the energy density per volume (E^2) by $\sigma' \approx E^2 A$. Using this relation, one finds the Schwinger production per length to be

$$\frac{\Gamma}{L} = \frac{\sigma'}{4\pi^3} e^{-\pi m_q^2/E} \ . \tag{2.2.2}$$

But what is this area? The radius of the flux tube is roughly given by [20]

$$R \sim \frac{1}{2} \frac{1}{\sqrt{\sigma'}} \ . \tag{2.2.3}$$

This allows one to find

$$E \sim \frac{\sqrt{\pi}}{2}\sigma' \ , \tag{2.2.4}$$

so that

$$\frac{\Gamma}{L} = \frac{\sigma'}{4\pi^3} e^{-\frac{2m_q^2}{\sigma'\sqrt{\pi}}} \approx \frac{\sigma'}{4\pi^3} e^{-\frac{2}{3.6\sqrt{\pi}}\left(\frac{m_q}{\Lambda_{\mathrm{QCD}'}}\right)^2} \ . \tag{2.2.5}$$

Hence, the probability of pair production is highly suppressed for quirks, whose masses are significantly above the confinement scale.

When determining the dynamics of the system, one must note that the quirks are produced at threshold, so they have almost zero separation. For quirks not produced at threshold, the nonzero separation means that some amount of energy is stored within the flux tube at production. However, this stored energy is smaller that the kinetic energy E_k and mass energy of the quirks. The three-momentum of a quirk is related to the velocity relativistically by

$$p = m_q \frac{v}{\sqrt{1-v^2}} \ , \tag{2.2.6}$$

so that the initial velocity of each quirk is

$$v_i = \frac{p}{\sqrt{p^2+m_q^2}} = \frac{\sqrt{E^2-m_q^2}}{E} = \sqrt{1-\frac{m_q^2}{E^2}} \ . \tag{2.2.7}$$

How the quirks' position evolves in time requires solving the relativistic version of Newton's second law

$$\frac{dp}{dt} = F = -\sigma' \ , \tag{2.2.8}$$

which, when integrated, becomes

$$\frac{v}{\sqrt{1-v^2}} = -\frac{\sigma'}{m_q}t + c_0 \ , \tag{2.2.9}$$

where c_0 is given by the initial velocity

$$c_0 = \frac{v_i}{\sqrt{1-v_i^2}} = \sqrt{\frac{E^2}{m_q^2}-1} \ . \tag{2.2.10}$$

The velocity is then

$$v(t) = \frac{\sqrt{E^2 - m_q^2} - \sigma' t}{\sqrt{m_q^2 + \left(\sqrt{E^2 - m_q^2} - \sigma' t\right)^2}} \ . \tag{2.2.11}$$

Since the quirks are bound, they move apart at gradually slower speeds until the velocity becomes zero at time

$$t = \frac{\sqrt{E^2 - m_q^2}}{\sigma'} \ . \tag{2.2.12}$$

This time is called a turning point. From the creation of the bound pair, one full period of oscillation is when the quirks move outward to zero velocity, back the other way to another turning point, and finally return to the initial configuration with the quirks moving apart once again. This period is given by

$$T = 4\frac{\sqrt{E^2 - m_q^2}}{\sigma'} \ , \tag{2.2.13}$$

so the angular frequency is

$$\omega = \frac{\pi\sigma'}{2\sqrt{E^2 - m_q^2}} \ . \tag{2.2.14}$$

As quirks are charged particles, this oscillatory motion leads to the radiation energy in the form of gauge bosons. The most notable of these emitted bosons are photons—which are easy to detect—and hidden gluons—which would lead to quicker de-excitation (and hence decay) times.

2.2.1 Photon Emission

Photons emitted during the oscillation of the quirk bound state (or quirkonium) are dominantly of the frequency given in Eqn. (2.2.14) [21]. This frequency also dictates the energy of these photons. Note that the emitted photons are quite soft—meaning that their energy is small—when the kinetic energy of the quirks is large.

The force between the quirks is simply

$$F = -\frac{dV}{dr} = -\sigma' \ , \tag{2.2.15}$$

which leads to an acceleration of $a = -\sigma'/m_q$. Using the relativistic generalization of the classical Larmor formula [22], the radiated power into massless gauge bosons is

$$\begin{aligned}\mathcal{P} &= \frac{8\pi\alpha}{3(1-v^2)^3}\left[a^2(1-v^2) + (\vec{v}\cdot\vec{a})^2\right] \\ &= \frac{8\pi\alpha\sigma'^2}{3m_q^2(1-v^2)^3}\ ,\end{aligned} \tag{2.2.16}$$

where the velocity and acceleration are assumed to always be either parallel or antiparallel.

Plugging in the velocity found in Eqn. (2.2.11), the radiated power is

$$\begin{aligned}\mathcal{P} =& \frac{8\pi\alpha\sigma'^2}{3m_q^2}\left[1 + \left(\sqrt{\frac{E^2}{m_q^2} - 1} - t\frac{\sigma'}{m_q}\right)^2\right]^3 \\ =& \frac{8\pi\alpha\sigma'^2 E^6}{3m_q^8}\left(1 - 2\frac{\sigma' t}{E}\sqrt{1 - \frac{m_q^2}{E^2}} + \frac{\sigma'^2 t^2}{E^2}\right)^3\ ,\end{aligned} \tag{2.2.17}$$

which can be integrated from $t = 0$ to the classical turning point. Doing so yields the energy radiated in one quarter period. The energy radiated over a full period is then

$$E_{\text{period}} = \frac{32\pi\alpha\sigma' E^7}{9m_q^8}\sqrt{1 - \frac{m_q^2}{E^2}}\left(1 + 2\frac{m_q^2}{E^2}\right)\ . \tag{2.2.18}$$

With these results the number of radiated photons in one period can be estimated

$$N_\gamma = \frac{E_{\text{period}}}{\omega} = \frac{64\alpha}{9}\left(\frac{E}{m_q}\right)^8\left(1 - \frac{m_q^2}{E^2}\right)\left(1 + 2\frac{m_q^2}{E^2}\right)\ . \tag{2.2.19}$$

If $N_\gamma < 1$, it can be thought of as the probability to radiate a photon. As energy decreases, the probability also decreases. For $v_i < 0.85$ the energy is $E \lesssim 2m_q$. The time for the pair to de-excite to the ground state ($E - m_q \sim 0$) is

$$t_{\text{de-excite}} \sim \frac{E - m_q}{\mathcal{P}} = \frac{3m_q^2(E - m_q)}{8\pi\alpha\sigma'^2}\ . \tag{2.2.20}$$

This result, together with $E = 7m_q/6$, agrees well with more precise calculations.[2]

[2]Other discussions of de-excitation can be found in [23, 24].

2.2.2 Glueball Emission

Several key distinctions between the radiation of photons and the radiation of gluons require that the two to be treated differently. First is that while a single photon can be radiated with frequency dictated by the the bound state's oscillations, a gluon cannot be radiated in isolation, since it is not a color singlet. Hence, there must be at least two emitted, forming a glueball with mass $m_0 \geq 6.8\Lambda_{\mathrm{QCD}'}$. Thus, it would make sense for the glueball radiation to go like α_s^2, instead of just α_s, and to be suppressed by ω/m_0 to some power. However, for quirks produced with large kinetic energy the first few oscillations radiate a lot of energy, which could be enough for glueball production.

Others seem to assume that this is far too unlikely to happen, though what remains to be shown is how unlikely it is. This assumption can be avoided by considering when the quirks pass by one another within a region with radius $\Lambda_{\mathrm{QCD}'}^{-1}$. This region contains what is in essence a large gluon background field.[3] What this means is that multiple gluons can be radiated without any loss to the quirkonium system. Relevant scales in this region are $\Lambda_{\mathrm{QCD}'}$ and the glueball mass, so the classical oscillation frequency does not play a role.

The radiation of a hard gluon, one with enough mass to produce a glueball, is given by a diagram for the process $qq \to qqg$, in which two on-shell quirks or squirks (scalar quirks) pass each other and radiate a hard gluon. For the scattering amplitude to be nonzero, the quirks must exchange an off-shell gluon, connected to an off-shell quirk. This virtual quirk radiates the hard gluon in order to go on-shell. Such a diagram leads one to expect that the amplitude scales like m_0^{-6} or m_0^{-8} for a fermionic or scalar quirk, respectively. Perhaps one can estimate how this process scales with the energy and mass of the quirks and with the confinement scale.

[3]This region is known as the "brown muck" region, due to the many colored gluons continually interacting.

From Eqn. (2.2.19), it can be seen that the first few periods release many photons when the energy of the quirks is much larger than their mass. If one considers this to be similar to the radiation of gluons, can enough gluon energy be emitted within a time of $t_{\mathrm{QCD}'} = \Lambda_{\mathrm{QCD}'}^{-1}$ to produce a glueball? In this scenario, the number of gluballs would be

$$N_{GB} = \frac{E_{\mathrm{period}}}{m_0}\frac{t_{\mathrm{QCD}'}}{T} = 0.53\frac{8\pi\alpha_s\sigma' E^6}{9m_q^8}\left(1 + 2\frac{m_q^2}{E^2}\right) \ . \tag{2.2.21}$$

At large energy, this number could be enhanced by as much as 2^6. However, it is suppressed by $\Lambda_{\mathrm{QCD}'}^2/m_q^2 \sim 10^{-4}$. Therefore, during the oscillation process before decay, glueball emission seems unlikely.

Chapter 3

Production Calculations

Quirks are produced in bound states (called "quirkonium"), meaning that the production from a collider event involves computing the scattering cross sections for quark-quark to quirk-quirk using Feynman diagrams and quantum field theory (QFT) calculations. While the specific details of calculations will be omitted, the results and necessary equations are included for the production of charged squirkonium (bound scalar quirks with net electric charge). Additionally, since the LHC collides protons (which are composite particles), proper calculation of cross sections and comparison with experimental searches requires evaluating how much each individual quark contributes to the interaction.

3.1 Production Cross Sections

The most straightforward part of the process is calculating the cross section for scalar quirks (or "squirks") produced from quarks. This project focuses on analyzing squirks, though fermionic quirks will be considered in future work.

Squirks are assumed to carry a SM electric and weak charges, so they can couple to the photon and the W and Z bosons. However, they cannot directly couple to SM quarks and

gluons since they are charged under a different confining gauge group. Hence, for squirkonium produced with a net electric charge, the only process to consider for production is

$$q\bar{q}' \to W^{\pm} \to \tilde{q}\bar{\tilde{q}}' \ ,$$

where q represents a SM quark and $\tilde{q}$ represents a quirk. The leading-order Feynman diagram for this process is shown in Figure 3.1.

From the usual Feynman rules for the SM and generalizing those found in [25], the matrix elements for this diagram are

$$\begin{aligned} i\mathcal{M}_{\text{prod}} &= \left(\frac{-ig}{\sqrt{2}}\right)^2 \bar{v}(p_2)\gamma^{\mu}P_L u(p_1)\frac{-i}{k^2 - m_W^2}\left(\eta_{\mu\nu} - \frac{k_\mu k_\nu}{m_w^2}\right) c(p_u - p_d)^{\nu} \\ &= \frac{ig^2 c}{2(k^2 - m_W^2)}\bar{v}(p_2)\gamma^{\mu}P_L u(p_1)(p_3 - p_4)_{\mu} \ , \end{aligned} \tag{3.1.1}$$

where $g = e/\sin\theta_W$ is the electroweak coupling and c is a constant that relates the flavor mixing of the SM quarks and the flavor mixing of the squirks. For computational purposes, the constant is $|c| = 1$. The u and $\bar{v}$ are spinors (since quarks are fermions) which help in cancellation of the $k_\mu k_\nu$ term and, when summed over spin states of the fermions, yield

$$\sum_s u(p)\overline{u}(p) = \sum_s \overline{u}(p)u(p) = \not{p} + m \qquad \text{and} \qquad \sum_s v(p)\overline{v}(p) = \sum_s \overline{v}(p)v(p) = \not{p} - m \ . \tag{3.1.2}$$

Since, the cross section depends on the magnitude of the matrix elements squared (also called amplitude squared), one must calculate the magnitude squared and then average over

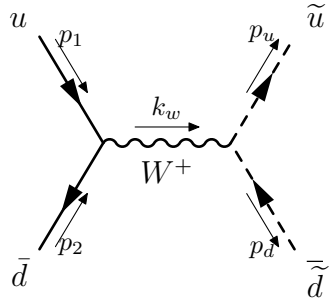

Figure 3.1 Leading-order Feynman diagram for positively charged squirkonium production.

initial spin states to get the quantity necessary. Using the Mandelstam variables

$$s \equiv (p_1 + p_2)^2 = (p_u + p_d)^2 \tag{3.1.3a}$$

$$t \equiv (p_1 - p_u)^2 = (p_2 - p_d)^2 \tag{3.1.3b}$$

$$u \equiv (p_1 - p_d)^2 = (p_2 - p_u)^2 \ , \tag{3.1.3c}$$

and the fact that $m_1, m_2 \ll m_u, m_d$,[1] it can shown the production amplitude is

$$|\overline{\mathcal{M}}_{\text{prod}}|^2 = \frac{1}{4}\sum_{s_1,s_2} |\mathcal{M}_{\text{prod}}|^2 = \frac{g^4|c|^2}{4(s - m_w^2)^2}(tu - m_u^2 m_d^2) \ . \tag{3.1.4}$$

Equivalently, if one considers the center-of-momentum (CM) frame, the $(tu - m_u^2 m_d^2)$ can be written in terms of the three-momentum of an individual squirk (since their three-momenta are equal and opposite in the CM frame) and the opening angle between the squirks. In this case, the amplitude becomes

$$|\overline{\mathcal{M}}_{\text{prod}}|^2 = \frac{1}{4}\sum_{s_1,s_2} |\mathcal{M}_{\text{prod}}|^2 = \frac{g^4|c|^2}{4(s - m_w^2)^2}|\vec{p}_f|^2 \sin^2\theta \ . \tag{3.1.5}$$

A standard cross section calculation ($2 \to$ many) utilizes the formula

$$d\sigma = \frac{|\overline{\mathcal{M}}(p_1 p_2 \to p_f)|^2}{(2E_1)(2E_2)|\vec{v}_1 - \vec{v}_2|} d\Pi_{\text{LIPS}} \ , \tag{3.1.6}$$

where $d\Pi_{\text{LIPS}}$ is a product of Lorentz-invariant phase space differential volume elements. For the special case of $2 \to 2$ scattering in the CM frame, this can be simplified to[2]

$$\left(\frac{d\sigma}{d\Omega}\right)_{\text{CM}} = \frac{|\overline{\mathcal{M}}(p_1 p_2 \to p_f)|^2}{(8\pi)^2 E_{\text{CM}}^2} \frac{|\vec{p_f}|}{|\vec{p_i}|}\theta(E_{\text{CM}} - m_3 - m_4) \ , \tag{3.1.7}$$

where $|\vec{p_i}|$ and $|\vec{p_f}|$ are the magnitudes of the initial and final state three-momenta. Using the matrix elements from Eqn. (3.1.5), the differential cross section can be integrated to get

$$\sigma(u\bar{d} \to \widetilde{u}\overline{\widetilde{d}}) = \frac{g^4|c|^2}{48\pi} \frac{|\vec{p}_f|^3}{\sqrt{s}(s - m_w^2)^2} \ . \tag{3.1.8}$$

[1] In this limit the quarks can be treated as massless to simplify the calculations.

[2] Several standard QFT textbooks make this derivation, such as [14, 26].

Since the diagram for $d\bar{u} \to W^- \to \widetilde{d}\widetilde{\bar{u}}$ will look similar, this process can be followed to get the same cross section for negatively charged squirkonium. All that remains in calculating the production cross sections is to deal with the quark side of things.

3.2 Parton Distribution Functions

Section 2.1 discussed how protons are made up of partons and how those partons can pair produce. Since the LHC was designed to accelerate and collide protons, one must consider how much of a role each of the constituent partons plays in any given collision. In the SM, quarks can couple in groups of two (called mesons) or three (called baryons) by way of the strong force's mediator, the gluon.

The proton is a baryon and many textbooks list the proton as being made up of two up quarks and a down quark[3], and this matches very well with experiment. However, this is not the full truth. In fact, the proton is a mess of various quarks and gluons constantly interacting. The up and down quarks are the "valence" quarks within the proton, while the others are denoted "sea" quarks. Valence quarks carry more of a hadron's momentum than sea quarks. How the quarks and gluons are distributed within a hadron is called a parton distribution function (PDF). These PDFs are determined primarily from experimental data and are necessary in computing cross sections for processes involving hadrons–such as those where protons are the initial states like at the LHC.

A standard set of PDFs used in these computations is known as the MSTW PDFs [29], named after A.D. Martin, W.J. Stirling, R.S. Thorne, and G. Watt, who published the set. Using Mathematica, the PDF data was read into a notebook and used to construct grids for the PDFs relating to the up and down quarks and their antiparticles, since those quarks contribute to the charged squirkonium production. The contributions from other generations

[3]See [27] or [28] for examples.

of quarks are small because of the PDFs for a proton. Since the grids are made using a discrete number of points, it is necessary to create interpolation of the grids. These PDF interpolations are then used to construct luminosity grids and corresponding interpolations, which are then convolved with the production cross section $\widehat{\sigma}$ which was calculated in Section 3.1 to give the overall cross section for the process.

For a given interaction, luminosities are made by convolving the PDFs of partons m and n at a factorization scale $\mu_F = \tau S$ which separates short- and long-range effects of the partons. For protons with four-momenta p_1 and p_2, the Mandelstam variable $S = (p_1 + p_2)^2$ is the same as the CM energy squared of the collider. The other piece, $\tau = s_{\text{parton}}/S$, can be thought of as the part of the protons' CM energy that actually contributes to the partonic interaction, since it relates the Mandelstam variables (and hence CM energies) of the partons and the protons. The luminosity is then computed as

$$\frac{dL_{mn}}{d\tau} = \int_\tau^1 \frac{dx}{x} \frac{1}{1+\delta_{mn}} \left[f_m(x,\mu_F) f_n(\frac{\tau}{x},\mu_F) + f_n(x,\mu_F) f_m(\frac{\tau}{x},\mu_F) \right] . \tag{3.2.1}$$

Defining $\widehat{\sigma}(mn \to \widetilde{q}\overline{\widetilde{q}}')$ as the cross section computed from Feynman diagrams (such as in Section 3.1), the overall cross section for $pp \to \widetilde{q}\overline{\widetilde{q}}'$ is then

$$\sigma = \int_{\tau_0}^1 d\tau \frac{dL_{mn}}{d\tau} \widehat{\sigma}(\tau S, \alpha_s(\mu_R)) \tag{3.2.2}$$

where μ_R is the renormalization scale, which is around the mass of the squirks. This result enables comparison with experimental searches, as it describes the likelihood that squirks could be produced in a proton-proton collision (or any hadron-hadron collision, for that matter).

Chapter 4

Decay and Experimental Searches

For the case of squirkonium with nonzero electric charge, there are two types of decay product possibilities to consider: it can either β-decay into neutral squirkonium or it can produce signals consisting of fermions or a W boson and another boson. Understanding the former will help in determining whether or not one needs to consider the neutral bound states in the analysis of the charged production. Decay signals, on the other hand, are what could be measured in a detector. Hence, understanding the probability of how often a charged bound state decays into each signal will be crucial in determining detection strategies. These probabilities are called branching fractions or branching ratios.

4.1 Beta Decay

In electroweak theory, any bound state with electroweak charge can, in principle, shed some of its charge through β-decay. Since quirks have nonzero electric charge and can also interact through W boson, the possibility for charged squirkonium to β-decay exists. The question one must ask, then, is how does the time scale for β-decay compare to the time to de-excite and decay into charged signals?

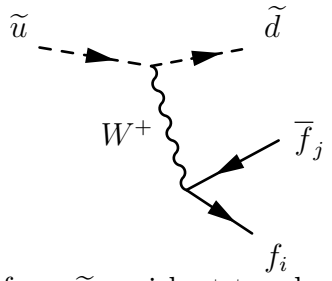

Figure 4.1 Three-body decay for a $\widetilde{u}$ squirk at tree-level. A similar diagram can be computed for the decay of the $\widetilde{d}$ squirk.

When the mass splitting between squirks is less than the mass of the W, the bound squirks cannot immediately decay into a W. Hence, for a bound state with electric charge $\pm e$ to shed its charge, it must decay through an off-shell W to a neutral state with a fermion-antifermion pair carrying away the excess charge. This can be modeled by simply considering the three-body decay of one squirk, shown in Figure 4.1. At tree-level, the matrix elements for this process are

$$i\mathcal{M}_\beta = \frac{-ie^2 c\xi_{ij}}{\sin^2\theta_W\,(2p_i\cdot p_j - m_w^2)}\overline{u}(p_i)\not{p}_u P_L v(p_j)\ , \tag{4.1.1}$$

where ξ_{ij} is a constant that takes into account the mixing of the fermion flavors. The decay width is computed by integrating the matrix elements

$$\Gamma_\beta = \frac{1}{2m_u}\int D|\overline{\mathcal{M}}_\beta|^2\ . \tag{4.1.2}$$

The differential factor D, which usually includes products of d^3p_f/E_f with some delta functions and normalization factors, can be simplified in this case to be[1]

$$D = \frac{dE_i dE_j}{32\pi^3}\ . \tag{4.1.3}$$

Since the masses of the squirks in consideration are much larger than the masses of the fermions produced in this process, the bounds on the integrals over fermion energies can be

[1]See [30] for an example of this process.

found (with some algebra) to be

$$0 \leq E_i \leq \frac{m_u^2 - m_d^2}{2m_u} \ , \tag{4.1.4a}$$

$$\frac{m_u(m_u - 2E_i) - m_d^2}{2m_u} \leq E_j \leq \frac{m_u(m_u - 2E_i) - m_d^2}{2(m_u - 2E_i)} \ . \tag{4.1.4b}$$

Rewriting this in terms of the mass splitting ($\Delta = m_u - m_d$) and the total mass ($M = m_u + m_d$) of the squirks yields

$$0 \leq E_i \leq \frac{M\Delta}{M + \Delta} \tag{4.1.5a}$$

$$\frac{M\Delta - E_i(M + \Delta)}{M + \Delta} \leq E_j \leq \frac{M\Delta - E_i(M + \Delta)}{M + \Delta - 4E_i} \ . \tag{4.1.5b}$$

Expanding both the integrand and the bounds in a power series in terms of $\delta \equiv \Delta/M$, one finds (setting $|c|^2\xi_{ij}^2 \approx 1$)

$$\Gamma_\beta = \frac{G_F^{\,2} M^5 \delta^5}{15\pi^3} + \mathcal{O}(\delta^6) = \frac{G_F^{\,2}\Delta^5}{15\pi^3} + \mathcal{O}\left(\frac{\Delta^6}{M^6}\right) \ , \tag{4.1.6}$$

which exactly matches the results found in [23]. Then the lifetime for this process is

$$t_\beta = \frac{1}{\Gamma_\beta} \approx \frac{15\pi^3}{G_F^2\Delta^5} = \frac{30\pi m_w^4 \sin^4\theta_W}{\alpha^2\Delta^5} \tag{4.1.7}$$

Comparing this to the de-excitation time from photon emission,

$$\frac{t_\beta}{t_{\text{de-excite}}} = \frac{30\pi m_w^4 \sin^4\theta_W}{\alpha^2\Delta^5} \times \frac{8\pi\alpha\sigma'^2}{3m_u^2(E - m_u)} \tag{4.1.8}$$

Following the approximation $E \lesssim 2m_u$ from Section 2.2.1 and making the substitution $m_u = \frac{1}{2}(M + \Delta)$, this ratio simplifies to

$$\frac{t_\beta}{t_{\text{de-excite}}} \gtrsim \frac{10^5 m_w^4 \Lambda_{\text{QCD}'}^2}{\Delta^5(M + \Delta)^3} \tag{4.1.9}$$

This ratio is large for small mass splitting, so the squirkonium will de-excite before it can β-decay. On the other hand, since the squirk masses are much larger than the confinement scale, a mass splitting of $\Delta \approx M$, which would normally be the upper limit in another theory,

is not allowed. Picking a total mass of $M = 500$ GeV, a mass splitting of $\Delta = m_w$ and a confinement scale of $\Lambda_{\mathrm{QCD}'} = 100$ MeV leads to a minimum ratio of around

$$\frac{t_\beta}{t_{\text{de-excite}}} \sim 10^{-8} \ . \tag{4.1.10}$$

This ratio is fairly small, but when $\Delta \geq m_w$ squirkonium could radiate an on-shell W (and another boson) instead of normal β-decay.

4.2 Branching Ratios

Section 4.1 showed that a bound pair of squirks with a net electric charge will de-excite and annihilate in the charged bound state. This means that all the decay states available are either viable signals that could be measured in a detector or are signals in the hidden sector. Of the viable signals, there are only two signals of interest—the $W\gamma$ signal and the WZ signal. Two other signals that do not contribute but warrant some discussion are the decays to fermions and the WH signal. Branching ratios are then constructed according to the equation

$$BR = \frac{\Gamma_j}{\Gamma_{\text{tot}}} = \frac{\Gamma_j}{\sum_{\text{i}} \Gamma_i} \ , \tag{4.2.1}$$

where Γ is the decay width for a particular signal. Using a formula for squirkonium decay widths from [31], these decay widths are given by

$$\Gamma(\widetilde{q}_1 \overline{\widetilde{q}}_2 \to ij) = \frac{3}{32\pi^2(1+\delta_{ij})} \frac{|R(0)|^2}{M^2} \beta_{ij} |\overline{\mathcal{M}}_{ij}|^2 \ , \tag{4.2.2}$$

with $R(0)$ being the radial wavefunction of the bound state at the origin, $|\overline{\mathcal{M}}_{ij}|^2$ being the amplitude squared for the given process, and β_{ij} being the final state velocity given by

$$\beta_{ij} = \sqrt{\left(1 - \frac{m_i^2 + m_j^2}{M^2}\right)^2 - 4\frac{m_i^2 m_j^2}{M^4}} \ . \tag{4.2.3}$$

All that remains is to find the amplitudes for the processes. After determining the amplitudes (and hence the branching ratios), the production cross section found in Section 3.1 need only be multiplied by each of the branching ratios to determine the total cross section for each signal.

For the case of squirkonium decaying at low angular momentum (i.e. zero relative velocity), the relevant signals are only the $W\gamma$ and WZ. These amplitudes were calculated analytically and the resulting branching ratios for various values of mass splitting can be found in Figure 4.2. It should be noted that the results asymptotically approach those of [23], where $\Delta = 0$ and $M = 1000$ GeV, but consider the more general scenario when the squirks do not have the same masses. For that mass splitting, the $W\gamma$ signal would carry the most weight in search strategies for quirk models with degenerate masses. The drastic change in branching fractions between the $\Delta = 0$ and $\Delta = m_w/2$ curves is something that will be explored to determine if there is any physical significance.

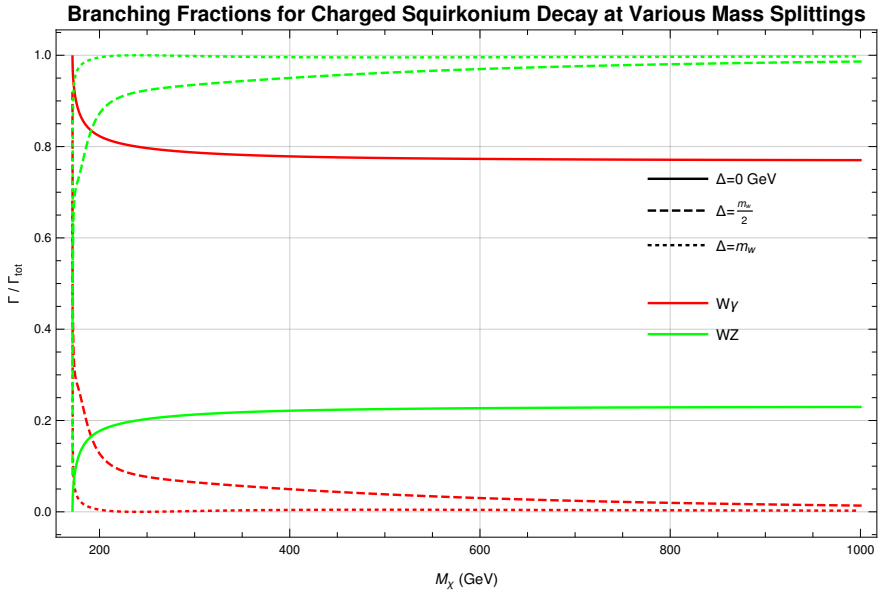

Figure 4.2 Branching ratios for squirkonium decay at low angular momentum with mass splittings $\Delta = 0$, $\Delta = \frac{m_w}{2}$, and $\Delta = m_w$.

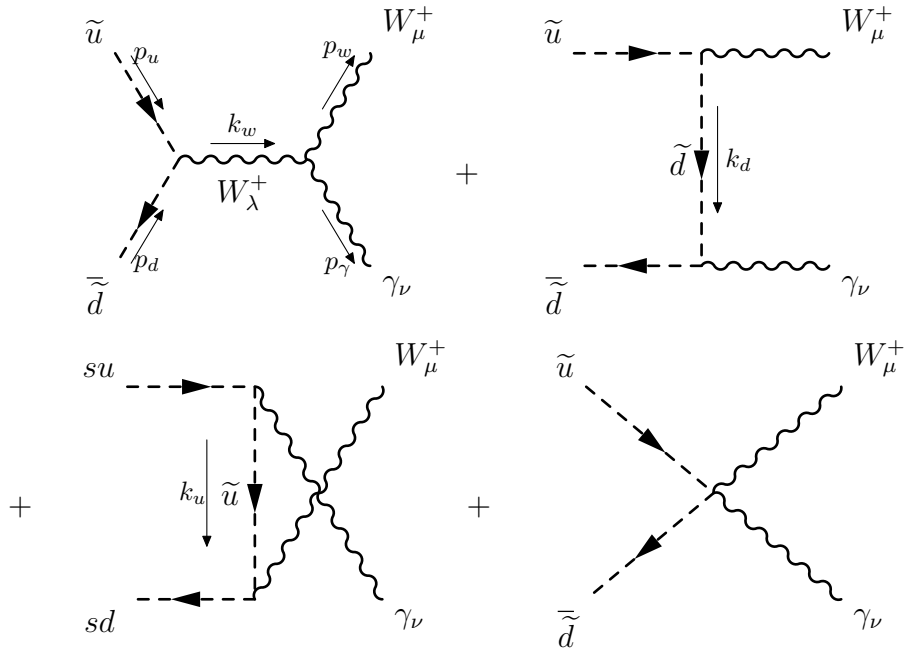

Figure 4.3 The four tree-level diagrams contributing to positively charged squirkonium decaying into $W^+ + \gamma$.

4.2.1 Search Signals

$W\gamma$ Signal

Of the signals, the first and most interesting one to consider for models with squirks of equal mass is the $W + \gamma$ final product states. Section 4.2 showed that this signal is the most probable in such models. At tree level, there are four diagrams (shown in Figure 4.3 for positively charged squirkonium) that contribute to this process: the s-, t-, and u-channels, as well as a 4-point vertex. After some work and by using some properties of the polarization

vectors, the matrix elements for each of the diagrams are

$$i\mathcal{M}_s(W\gamma) = \frac{-ie^2c}{\sqrt{2}\sin\theta_W(p_w\cdot p_\gamma)}(g^{\mu\nu}(p_\gamma\cdot(p_u-p_d)) + 2(p_u^\mu p_d^\nu - p_d^\mu p_u^\nu)) \ , \tag{4.2.4a}$$

$$i\mathcal{M}_t(W\gamma) = \frac{-2iq_de^2c}{\sqrt{2}\sin\theta_W(p_d\cdot p_\gamma)}p_u^\mu p_d^\nu \ , \tag{4.2.4b}$$

$$i\mathcal{M}_u(W\gamma) = \frac{-2iq_ue^2c}{\sqrt{2}\sin\theta_W(p_u\cdot p_\gamma)}p_d^\mu p_u^\nu \ , \tag{4.2.4c}$$

$$i\mathcal{M}_4(W\gamma) = \frac{i(q_u+q_d)e^2c}{\sqrt{2}\sin\theta_W}g^{\mu\nu} \ . \tag{4.2.4d}$$

where the q_u and q_d are the electric charges of the up and down squirks (with $q_u - q_d = 1$, so that charge is conserved in the production of the W). Adding Eqns. (4.2.4) together, the full matrix element for the process $\widetilde{u}\overline{\widetilde{d}} \to W^+\gamma$ becomes

$$i\mathcal{M}_{W\gamma} = \frac{ie^2c\epsilon_\mu^{w*}\epsilon_\nu^{\gamma*}}{\sqrt{2}\sin\theta_W}\left(A_{W\gamma}p_d^\mu p_u^\nu + B_{W\gamma}p_u^\mu p_d^\nu + C_{W\gamma}g^{\mu\nu}\right) \ , \tag{4.2.5}$$

with coefficients

$$A_{W\gamma} \equiv 2\left(\frac{1}{p_w\cdot p_\gamma} - \frac{q_u}{p_u\cdot p_\gamma}\right) \ , \tag{4.2.6a}$$

$$B_{W\gamma} \equiv -2\left(\frac{1}{p_w\cdot p_\gamma} + \frac{q_d}{p_d\cdot p_\gamma}\right) \ , \tag{4.2.6b}$$

$$C_{W\gamma} \equiv \left(q_u + q_d - \frac{p_\gamma\cdot(p_u-p_d)}{p_w\cdot p_\gamma}\right) \ . \tag{4.2.6c}$$

Averaging over squirk colors, and summing over the external polarizations, the amplitude squared of the process is

$$|\overline{\mathcal{M}}_{W\gamma}|^2 = \frac{e^4|c|^2}{2\sin^2\theta_W}\left[m_um_d\left(A_{W\gamma}+B_{W\gamma}\right)\left(1-\frac{E_w^2}{m_w^2}\right)\right.$$
$$\left.\times\left(m_um_d\left(A_{W\gamma}+B_{W\gamma}\right)+2C_{W\gamma}\right)+3C_{W\gamma}^2\right] \ . \tag{4.2.7}$$

In the center-of-momentum frame and with the substitution $M = m_u + m_d$ and $\Delta = m_u - m_d$ (where it is assumed that $m_u \geq m_d$), this result simplifies nicely to

$$|\overline{\mathcal{M}}_{W\gamma}|^2 = \frac{e^4|c|^2}{\sin^2\theta_W}\left(q_u+q_d-\frac{\Delta}{M}\right)^2 \ . \tag{4.2.8}$$

This amplitude, together with the amplitude for the WZ was used to construct the branching fractions.

WZ Signal

The next interesting signal to consider is the $W + Z$ final product states. The Feynman diagrams for this process are similar to that of the $W\gamma$ signal seen in Figure 4.3 (for positively charged squirkonium), but with a Z boson instead of a photon.

The matrix elements also have a similar structure

$$i\mathcal{M}_{WZ} = \frac{ie^2 c\epsilon_\mu^{w*}\epsilon_\nu^{z*}}{\sqrt{2}\sin^2\theta_W\cos\theta_W}\left(A_{WZ}p_d^\mu p_u^\nu + B_{WZ}p_u^\mu p_d^\nu + C_{WZ}g^{\mu\nu}\right) \ , \tag{4.2.9}$$

with coefficients

$$A_{WZ} \equiv 2\left(\frac{2\cos^2\theta_W}{m_z^2 + 2p_w\cdot p_z} + \frac{|Z_u|^2 - 2q_u\sin^2\theta_W}{m_z^2 - 2p_u\cdot p_z}\right) \ , \tag{4.2.10a}$$

$$B_{WZ} \equiv -2\left(\frac{2\cos^2\theta_W}{m_z^2 + 2p_w\cdot p_z} - \frac{|Z_d|^2 + 2q_d\sin^2\theta_W}{m_z^2 - 2p_d\cdot p_z}\right) \ , \tag{4.2.10b}$$

$$C_{WZ} \equiv -(q_u + q_d)\sin^2\theta_W - \frac{\cos^2\theta_W}{m_z^2 + 2p_w\cdot p_z}\left(2p_z\cdot(p_u - p_d) - \frac{m_z^2}{m_w^2}(m_u^2 - m_d^2)\right) \ , \tag{4.2.10c}$$

where the new parameters Z_u and Z_d are the matrix elements related to the coupling of the Z to the up and down squirks, respectively. For computational purposes, these matrix elements were set to have a magnitude of 1.

Averaging over squirk colors, and summing over the external polarizations, the amplitude squared of the process becomes (after making the substitution to M and Δ)

$$\begin{aligned}|\overline{\mathcal{M}}_{WZ}|^2 = \frac{e^4|c|^2}{32\sin^4\theta_W\cos^2\theta_W}\Bigg[&D_{WZ}\left(1 - \frac{E_w^2}{m_w^2} - \frac{E_z^2}{m_z^2}\right)(D_{WZ} + 8C_{WZ}) + 32C_{WZ}^2 \\ &+ \frac{1}{m_w^2 m_z^2}\left(D_{WZ}E_wE_z + 2C_{WZ}(M^2 - m_w^2 - m_z^2)\right)^2\Bigg] \ ,\end{aligned} \tag{4.2.11}$$

where in the CM frame the constants are given by

$$\begin{aligned} D_{WZ} &= (M^2 - \Delta^2)(A_{WZ} + B_{WZ}) \\ &= 2(M^2 - \Delta^2)\left(\frac{|Z_u|^2 - 2q_u \sin^2\theta_W}{m_z^2 - E_z(M+\Delta)} - \frac{|Z_d|^2 + 2q_d \sin^2\theta_W}{m_z^2 - E_z(M-\Delta)}\right) , \end{aligned} \tag{4.2.12a}$$

$$C_{W\gamma} = -\sin^2\theta_W \left(q_u + q_d + \frac{\Delta}{M}\right) . \tag{4.2.12b}$$

The amplitudes for the $W\gamma$ and WZ signals were the only two signals used to construct the branching fractions. There are two other signals, however, that one could imagine might contribute. The reasons for why they do not will be discussed next.

4.2.2 Other Signals

WH Signal

The first up in the discussion of signals is the W boson and a Higgs. While this signal conserves charge, one must also remember that from the discussion in Section 2.2 that bound quirks de-excite quickly and decay in the lowest angular momentum state, $\ell = 0$. It follows that the $W + H$ decay product, which has spin $\mathbf{1} \otimes \mathbf{0} = \mathbf{1}$, is suppressed for the case of scalar quirkonium decaying with no excess angular momentum.

Decay to Fermions

The other signal that does not contribute to potential search strategies is the decay into SM fermions. Squirks are assumed to not couple to SM fermions. Hence, the only diagram that can contribute at tree-level for the process $\widetilde{u}\overline{\widetilde{d}} \to f_i \overline{f}_j$ is the s-channel decay through a W^+ as shown in Figure 4.4. The matrix elements for the process are similar to that of production

$$i\mathcal{M} = i\frac{g^2 c}{2(k^2 - m_w^2)} v(p_j)\gamma_\mu P_L \bar{u}(p_i)(p_u - p_d)^\mu. \tag{4.2.13}$$

Summing over the spin states of the fermions and over the number of possible fermion combinations, $N_f = 12$, the amplitude (squared) can be found to be

$$|\overline{\mathcal{M}}_{\text{fermions}}|^2 = \frac{2g^4|c|^2 s}{(s - m_w^2)^2}|\vec{p}_u|^2 \sin^2\theta \ , \tag{4.2.14}$$

where $s = (p_u + p_d)^2$ is the Mandelstam variable and θ is the opening angle between the produced fermions. Since the squirkonium decays at low angular momentum, $|\vec{p}_u| \to 0$, so $|\overline{\mathcal{M}}_{\text{fermions}}|^2 \to 0$, meaning that the cross section is suppressed. Hence, the fermionic signal does not need to be considered in search strategies.

4.3 Resonance Searches at the LHC

The signals discussed in this chapter are more than just wishful thinking. In fact, the LHC has already searched for resonances in $W\gamma$ signal [32–35]. In these searches, no peaks have been found outside two standard deviations from the SM bounds. Comparing the searches, however, one finds that some searches are more sensitive than others. Indeed, Figure 4.5 shows that the ATLAS 8 TeV search has been the most sensitive among all the searches done for the $W\gamma$ resonance. Despite this, the fact that even the 8 TeV search has not revealed any new physics could mean that the searches are not sensitive enough to detect new states.

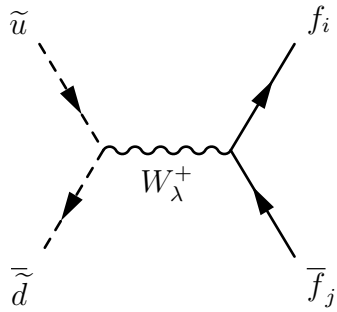

Figure 4.4 Only the s-channel contributes at tree-level to charged squirkonium decay into fermions.

For no mass splitting, the production cross section for a charged bound state could be detected (assuming the sensitivity of the 8 TeV search) up until a total mass $M \approx 640$ GeV. Newer searches are at higher luminosities and higher energies, but are too insensitive to this production. The decrease in sensitivity comes from a lack of resolution for the boosted decay products of the W boson—which are the hadronic final states. Then, as the LHC moves to upgrade its center-of-momentum energy and luminosity, the decay channels for the W will be even more boosted. Hence, the need to correlate different signals (such as $W\gamma$ and WZ) and correlate the decay channels for the massive bosons becomes even more important.

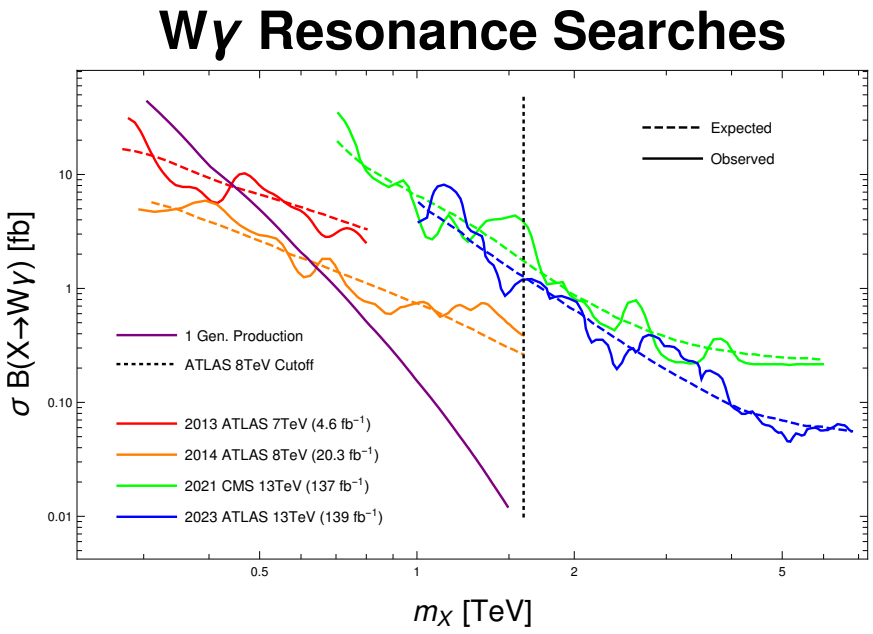

Figure 4.5 LHC resonance searches for the $W\gamma$ signal with the production cross section for squirks overlaid.

Chapter 5

Conclusions and Future Work

As colliders become more sensitive and reach higher energies, the question remains if there might be new physics currently being missed. The LHC, as the world's largest accelerator facility, continues its searches for signals that could potentially hint at the existence of quirks or squirks. Indeed, there could be squirk states sitting at energies already accessible to the LHC in its $W\gamma$ resonance searches, but the detectors are not able to resolve any resonances due to the boosted hadronic final states of the W. Such states could provide at least partial solutions to the electroweak hierarchy problem by approximately cancelling divergences that arise from the Higgs' coupling to SM particles such as the top quark.

The process considered in this work was for electrically charged squirkonium in the neutral naturalness framework. It showed that the production and decay of charged squirkonium (with no mass splitting between squirks) into a $W\gamma$ signal only exceeds the LHC's most sensitive search until a total mass of around $M \lesssim 640$ GeV. This same process can be adapted to other types of quirky bound states (scalar or fermionic, charged or neutral).

While this research focused on comparing the charged squirkonium production and decay to experimental searches conducted for $W\gamma$ resonances, it remains to be seen how much the sensitivity of resonance searches can be improved by taking into account the different

decay channels of the W. Since the searches were done using hadronic final states, perhaps including the fermionic states could lead to a noticeable gain in sensitivity.

Another route to improve search techniques could be to find a way to correlate the $W\gamma$ and WZ signals. Hence, the next step is to compare the experimental WZ resonance searches to the cross section for charged squirkonium decaying into said signal. Since the branching ratio for the WZ is less than that for $W\gamma$ (in the case of no mass splitting), developing a search strategy that could leverage both of these signals would lead to better chances of finding these states.

Since squirks could also form neutral bound states, a natural extension from charged squirkonium would be to consider the production and decay of neutral squirkonium. There are many more options for decay signals in such cases. These signals (e.g. $\gamma\gamma$, ZZ, $Z\gamma$, $f\bar{f}$, etc.) also have experimental searches to which the cross sections can be compared. Fermionic quirks will also be considered in like manner.

All of the types of signals explored above have only considered direct detection. Another interesting possibility is that the quirkonium decays through hidden glueballs, which later decay into something visible. These types of signals are called displaced decays and are also worth considering in future work. Others have created tools [36,37] that could help with that endeavor.

Bibliography

[1] G. Aad *et al.*, "Observation of a new particle in the search for the Standard Model Higgs boson with the ATLAS detector at the LHC," Phys. Lett. B **716,** 1–29 (2012).

[2] S. Chatrchyan *et al.*, "Observation of a New Boson at a Mass of 125 GeV with the CMS Experiment at the LHC," Phys. Lett. B **716,** 30–61 (2012).

[3] A. M. Sirunyan *et al.*, "Search for top quark partners with charge 5/3 in the same-sign dilepton and single-lepton final states in proton-proton collisions at $\sqrt{s} = 13$ TeV," JHEP **03,** 082 (2019).

[4] G. Aad *et al.*, "Search for a scalar partner of the top quark in the all-hadronic $t\bar{t}$ plus missing transverse momentum final state at $\sqrt{s} = 13$ TeV with the ATLAS detector," Eur. Phys. J. C **80,** 737 (2020).

[5] A. Tumasyan *et al.*, "Combined searches for the production of supersymmetric top quark partners in proton–proton collisions at $\sqrt{s} = 13\,\text{TeV}$," Eur. Phys. J. C **81,** 970 (2021).

[6] N. Craig, "Naturalness: A Snowmass White Paper," In *Snowmass 2021*, (2022).

[7] B. Batell, M. Low, E. T. Neil, and C. B. Verhaaren, "Review of Neutral Naturalness," In *Snowmass 2021*, (2022).

[8] G. Burdman, Z. Chacko, H.-S. Goh, and R. Harnik, "Folded supersymmetry and the LEP paradox," JHEP **02,** 009 (2007).

[9] L. B. Okun, "THETONS," Pisma Zh. Eksp. Teor. Fiz. **31,** 156–159 (1979).

[10] L. B. Okun, "THETA PARTICLES," Nucl. Phys. B **173,** 1–12 (1980).

[11] J. Kang and M. A. Luty, "Macroscopic Strings and 'Quirks' at Colliders," JHEP **11,** 065 (2009).

[12] R. P. Feynman, "The behavior of hadron collisions at extreme energies," Conf. Proc. C **690905,** 237–258 (1969).

[13] R. P. Feynman, "Very high-energy collisions of hadrons," Phys. Rev. Lett. **23,** 1415–1417 (1969).

[14] M. E. Peskin and D. V. Schroeder, *An Introduction to quantum field theory* (Addison-Wesley, Reading, USA, 1995).

[15] J. Bulava, B. Hörz, F. Knechtli, V. Koch, G. Moir, C. Morningstar, and M. Peardon, "String breaking by light and strange quarks in QCD," Phys. Lett. B **793,** 493–498 (2019).

[16] B. Lucini, M. Teper, and U. Wenger, "Properties of the deconfining phase transition in SU(N) gauge theories," JHEP **02,** 033 (2005).

[17] B. Lucini, M. Teper, and U. Wenger, "Glueballs and k-strings in SU(N) gauge theories: Calculations with improved operators," JHEP **06,** 012 (2004).

[18] M. Teper, "Large N and confining flux tubes as strings - a view from the lattice," Acta Phys. Polon. B **40,** 3249–3320 (2009).

[19] P. D. Group *et al.*, "Review of Particle Physics," Progress of Theoretical and Experimental Physics **2020,** 083C01 (2020).

[20] P. Bicudo, N. Cardoso, and M. Cardoso, "Pure gauge QCD flux tubes and their widths at finite temperature," Nucl. Phys. B **940,** 88–112 (2019).

[21] R. Harnik and T. Wizansky, "Signals of New Physics in the Underlying Event," Phys. Rev. D **80,** 075015 (2009).

[22] J. D. Jackson, *Classical Electrodynamics* (Wiley, 1998).

[23] G. Burdman, Z. Chacko, H.-S. Goh, R. Harnik, and C. A. Krenke, "The Quirky Collider Signals of Folded Supersymmetry," Phys. Rev. D **78,** 075028 (2008).

[24] H.-C. Cheng, L. Li, E. Salvioni, and C. B. Verhaaren, "Singlet Scalar Top Partners from Accidental Supersymmetry," JHEP **05,** 057 (2018).

[25] J. Rosiek, "Complete set of Feynman rules for the MSSM: Erratum," (1995).

[26] M. D. Schwartz, *Quantum Field Theory and the Standard Model* (Cambridge University Press, 2014).

[27] B. R. Martin, *Nuclear and particle physics* (2009).

[28] M. Serway *et al.*, *Modern physics* (James Madison University, 2005).

[29] A. D. Martin, W. J. Stirling, R. S. Thorne, and G. Watt, "Parton distributions for the LHC," Eur. Phys. J. C **63,** 189–285 (2009).

[30] S. Coleman, in *Lectures of Sidney Coleman on Quantum Field Theory*, B. G.-g. Chen, D. Derbes, D. Griffiths, B. Hill, R. Sohn, and Y.-S. Ting, eds., (WSP, Hackensack, 2018).

[31] S. P. Martin, "Diphoton decays of stoponium at the Large Hadron Collider," Phys. Rev. D **77,** 075002 (2008).

[32] G. Aad *et al.*, "Measurements of $W\gamma$ and $Z\gamma$ production in pp collisions at $\sqrt{s}$=7 TeV with the ATLAS detector at the LHC," Phys. Rev. D **87,** 112003 (2013), [Erratum: Phys.Rev.D 91, 119901 (2015)].

[33] G. Aad *et al.*, "Search for new resonances in $W\gamma$ and $Z\gamma$ final states in pp collisions at $\sqrt{s} = 8$ TeV with the ATLAS detector," Phys. Lett. B **738,** 428–447 (2014).

[34] A. Tumasyan *et al.*, "Search for Wγ resonances in proton-proton collisions at s=13 TeV using hadronic decays of Lorentz-boosted W bosons," Phys. Lett. B **826,** 136888 (2022).

[35] G. Aad *et al.*, "Search for high-mass Wγ and Zγ resonances using hadronic W/Z boson decays from 139 fb^{-1} of pp collisions at $\sqrt{s} = 13$ TeV with the ATLAS detector," JHEP **07,** 125 (2023).

[36] D. Curtin, C. Gemmell, and C. B. Verhaaren, "Simulating Glueball Production in $N_f = 0$ QCD," (2022).

[37] A. Batz, T. Cohen, D. Curtin, C. Gemmell, and G. D. Kribs, "Dark Sector Glueballs at the LHC," (2023).